2024 International Conference on Simulation of Semiconductor Processes and Devices (SISPAD) | 979-8-3315-1635-2/24/$31.00 ©2024 IEEE | DOI: 10.1109/SISPAD62626.2024.10733161

Generalization of Fick's law and derivation of interface segregation parameters using microscopic atomic movements

Chihak Ahn
TCAD lab
Samsung Semiconductor Inc.
San Jose, CA, USA
chihak.ahn@samsung.com

Joohyun Jeon
[*]CSE Team,
Samsung Electronics
Hwaseong-si, Korea

Seungmin Lee
CSE Team,
Samsung Electronics
Hwaseong-si, Korea

Woosung Choi
TCAD lab
Samsung Semiconductor Inc.
San Jose, CA, USA

Dae Sin Kim
CSE Team
Samsung Electronics
Hwaseong-si, Korea

Nick E.B. Cowern
School of Engineering
Newcastle University
Newcastle upon Tyne, UK

[*] Computational Science & Engineering team

***Abstract*—Using a microscopic picture of atomic movement we rederived the Fick's diffusion flux equation which naturally includes all types of drift causing terms (e.g. electrical drift, stress driven movement, and binding energy related effects). With a similar method, two-phase segregation transfer rate and three-phase segregation trapping/emission rates are also defined with measurable or calculable quantities.**

***Index Terms*—Fick's law, segregation, diffusion, trapping, emission, two-phase segregation, three-phase segregation**

I. Introduction

As three-dimensional stacking is widely used in state-of-the-art semiconductor fabrication, accurate modeling of dopant trapping at interfaces or dopant movement across interfaces becomes critical to optimize the process conditions. However, the interface modeling, especially at the amorphous interface, is challenging due to the lack of carefully designed experimental data or established theoretical calculation methodology. Specifically the interface segregation model parameters lack corresponding quantities from the atomistic calculations. Therefore the segregation transfer rate has been determined somewhat arbitrarily without a supporting theory. To overcome such difficulties, we derived a microscopic interface segregation parameters using accessible physical quantities.

II. Theory and Models

A. Generalized Fick's law

As the first step, we re-derived the Fick's first law using the microscopic atomic movement. Let's consider an atomic hopping in a three-dimensional space as shown in Fig. 1. The net hopping rate of an impurity at position x is given by

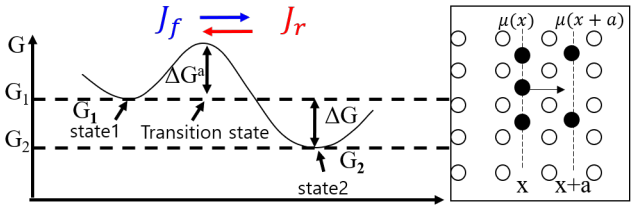

Fig. 1. Schematics of atomic hopping and free energy.

$$
\begin{aligned}
R &= k_f - k_r && (1)\\
&= \frac{\nu_0}{6}\exp\left(-\frac{\Delta G^a}{kT}\right)\left(1-\exp\left(-\frac{\Delta G}{kT}\right)\right) && (2)\\
&\approx \frac{\nu_0}{6}\exp\left(-\frac{\Delta G^a}{kT}\right)\frac{\Delta G}{kT} && (3)\\
&= \frac{\nu_0}{6}\exp\left(-\frac{\Delta G^a}{kT}\right)\frac{\mu(x+a)-\mu(x)}{kT} && (4)\\
&= \frac{\nu_0}{6}\exp\left(-\frac{\Delta G^a}{kT}\right)\frac{a}{kT}\frac{d\mu}{dx}, && (5)
\end{aligned}
$$

where ν_0 is the attempt frequency, ΔG^a the activation energy, ΔG $(G_1 - G_2)$ the free energy difference between the initial and the final state, a the hopping distance, kT the thermal energy, and μ the chemical potential. $\Delta G \ll kT$ is assumed in the approximation step which implies that the free energy of the impurity at stable position varies slowly in atomic hopping length scale. The flux to x direction is given by the product

of the areal impurity density($\sigma(x)$) and the hopping rate:

$$J_x = -\sigma(x)R, \tag{6}$$

$$= -\underbrace{\frac{\sigma(x)}{a}}_{c(x)}\underbrace{\frac{a^2\nu_0}{6}\exp\left(-\frac{\Delta G^a}{kT}\right)}_{D}\frac{1}{kT}\frac{d\mu}{dx}, \tag{7}$$

$$= -Dc(x)\frac{d\mu}{dx}, \tag{8}$$

where $c(x)$ is the volume concentration of the impurity and D the diffusivity. The chemical potential can be expressed as [1]

$$\mu = \mu_0 + kT\log\left(\frac{c(x)}{c^{eq}(x)}\right), \tag{9}$$

$$c^{eq}(x) = c_0\exp\left(-\frac{g^f(x)}{kT}\right), \tag{10}$$

where μ^0 is the reference chemical potential, $c(x)$ the impurity concentration, $c^{eq}(x)$ the equilibrium impurity concentration, c_0 the allowed site density for the impurity, and g^f the formation Gibbs free enegy. Plugging Eq. 10 into Eq. 8 yields the generalized Fick's first law.

$$J_x = -Dc^{eq}(x)\frac{d}{dx}\left(\frac{c(x)}{c^{eq}(x)}\right). \tag{11}$$

In a uniform, homogeneous material, $g^f(x)$ and $c^{eq}(x)$ are constant throughtout the space and does not have any effect on diffusion. However, any spatial variation in c^{eq} can cause a drift of the impurity. More explicitly, g^f can include the electric potential energy of ionized impurity, the stress response energy, the energy due to the entropy of configuration, and the binding energy between the impurity and the host material. In diffusion simulation, the electrical drift effect is well known and it is usually treated as a separate term. Using the generalized form of the Fick's law (Eq. 11) all drift terms can be described by a single term $c^{eq}(x)$. Extending the concept of the electrical drift to cover other effects, Eq. 11 can be rewritten as:

$$c_{eq}(\vec{r}) = c_0\exp\left(-\frac{\Sigma_i q_i\phi_i(\vec{r})}{kT}\right), \tag{12}$$

$$\vec{J} = -D\exp\left(-\frac{\Sigma_i q_i\phi_i(\vec{r})}{kT}\right)\vec{\nabla}_r\left(\frac{c(\vec{r})}{\exp\left(-\frac{\Sigma_i q_i\phi_i(\vec{r})}{kT}\right)}\right), \tag{13}$$

where q_i is the generalized charge and $\phi_i(\vec{r})$ the corresponding generalized potential (see table I for details).

TABLE I
DRIFT CAUSING GIBBS FREE ENERGY TERMS

Formation free energy term	**charge(q_i)**	**potential($\phi_i(\vec{r})$)**
electric potential energy	electric charge	electric potential
stress response energy	activation volume	stress or pressue
binding energy	binding energy	pairing probability
T× entropy	temparature	entropy

B. Interface segregation parameters

Deriving the transfer rate at a material interface is similar to deriving the Ficks law. However, $\Delta G \ll kT$ assumption is no longer valid across the interface, where abrupt changes of any physical quantity are allowed. To describe such conditions, the impurity concentrations and the segregation factors need to be defined on each side as shown in Fig. 2. Furthermore, there are differences in hopping distance (a_1 and a_2) and the attempt frequency (ν_1 and ν_2) on two sides. Then the flux across the interface is given by

$$J_x = J_f - J_r, \tag{14}$$

$$= \sigma_1 k_f - \sigma_2 k_r, \tag{15}$$

$$= \sigma_1\frac{\nu_1}{6}\exp\left(-\frac{E_1+\Delta E^a}{kT}\right) - \sigma_2\frac{\nu_2}{6}\exp\left(-\frac{E_1+\Delta E^a+G_2-G_1}{kT}\right), \tag{16}$$

$$= \frac{D_1}{a_1}\exp\left(-\frac{\Delta E^a}{kT}\right) \times\left(C_1 - \frac{a_2\nu_2}{a_1\nu_1}C_2\exp\left(-\frac{\Delta G}{kT}\right)\right), \tag{17}$$

$$= \frac{D_1}{a_1}\exp\left(-\frac{\Delta E^a}{kT}\right)\left(C_1 - \frac{a_2\nu_2}{a_1\nu_1}\frac{C_2}{s_2/s_1}\right), \tag{18}$$

where $D_1(D_2)$ is the diffusivity of the impurity in material-1 (material-2), $C_1(C_2)$ the concentration of the impurity in material-1 (material-2), $s_1(s_2)$ the equilibrium solubility in material-1 (material-2), and ΔE^a the extra barrier. By comparing Eq. 18 with the conventional two-phase segregation rate [2], the two-phase segregation transfer rate (h) can be defined using measurable or calculable quantities.

$$h = \frac{D_1}{a_1}\exp\left(-\frac{\Delta E^a}{kT}\right). \tag{19}$$

When the hopping length and the attempt frequency are similar in both sides ($a_1 \sim a_2$ and $\nu_1 \sim \nu_2$), the transfer flux can be simplified to the conventional form [2].

$$J_x = h\left(C_1 - \frac{C_2}{s_2/s_1}\right), \tag{20}$$

Previously the transfer rate was usually chosen somewhat arbitrarily in diffusion simulations because it is an abstractized physical quantity without clear connection to measurable or calculable quantities. With more careful consideration of the interface energy diagram (Fig. 3), the transfer rate (h) can have a symmetric form like

$$h = \frac{\sqrt{D_1 D_2}}{a}\exp\left(-\frac{\Delta E^a}{kT}\right), \tag{21}$$

where $a \sim a_1 \sim a_2$ is assumed.

When there are traps at the interface, three-phase segregation model [3] should be used. Based on Fig 4, the flux equations can be derived as:

$$J_1 = J_1^f - J_1^r, \tag{22}$$

$$= \sigma_1 k_1^f\frac{\sigma_{Max}-\sigma_i}{\sigma_{Max}} - \sigma_i k_1^r\frac{C_1^{Sol}-C_1}{C^{Sol}}, \tag{23}$$

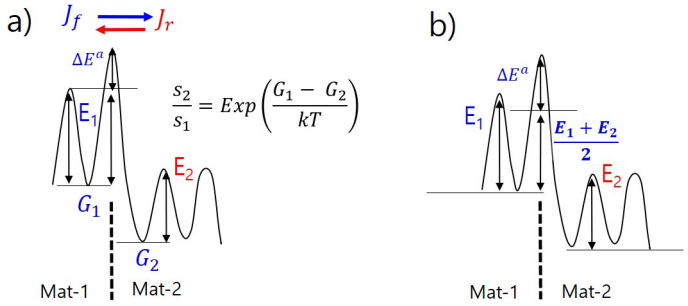

Fig. 2. Energy diagram for two-phase segregation using the E_1 as the activation barrier with an addition barrier ΔE^a (a) and the average value as the activation barrier (b).

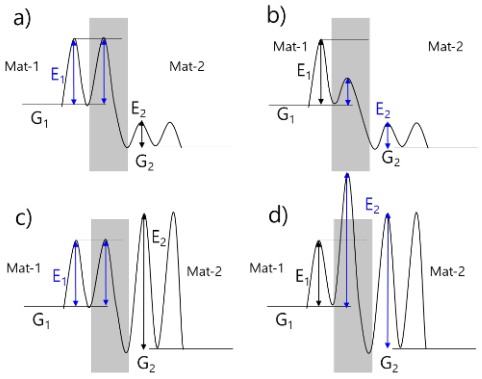

Fig. 3. Various configurations of energy diagrams at interface for two-phase segregation parameters. The case a) and c) depict the E_1 as the activation barrier and b) and d) represent the E_2 as the activation barrier. The two cases can be considered as the limiting cases and more reasonable choice would be the averaged value with an additional barrier as shown in Fig 2 b).

where σ_{Max} is the areal trap density at the interface, σ_i the occupied trap density, C_1^{Sol} the solubility of the impurity in material-1, C_1 the impurity concentration in material-1. Note that the trapping and emission fluxes in Eq. 23 are scaled by the available trap ratio $\left(\frac{\sigma_{Max}-\sigma_i}{\sigma_{Max}}\right)$ and the available soluble site ratio $\left(\frac{C_1^{Sol}-C_1}{C_1^{Sol}}\right)$, respectively.

$$J_1 = \sigma_1 \frac{\nu_1}{6} \exp\left(-\frac{E_1 + \Delta E_1^a}{kT}\right) \frac{\sigma_{Max} - \sigma_i}{\sigma_{Max}} - \sigma_i \frac{\nu_i}{6} \exp\left(-\frac{E_1 + \Delta E_1^a + G_1 - G_i}{kT}\right) \frac{C_1^{Sol} - C_1}{C_1^{Sol}}, \tag{24}$$

$$= \frac{D_1}{a_1 \sigma_{Max}} \exp\left(-\frac{\Delta E_1^a}{kT}\right) C_1 \left(\sigma_{Max} - \sigma_i\right) - \frac{D_1}{a_1^2 C_1^{Sol}} \frac{\nu_i}{\nu_1} \exp\left(-\frac{\Delta E_1^a + G_1 - G_i}{kT}\right) \sigma_i \left(C_1^{Sol} - C_1\right), \tag{25}$$

where σ_{Max} is the areal trap density of the interface, σ_i the areal trapped impurity density, C_1^{Sol} the solubility of the impurity in the material-1, C_1 the impurity concentration at material-1, ν_i the attempt frequency at the interface.

By comparing Eq.25 with [3], the key parameters can be defined as:

$$t_1 = \frac{D_1}{a_1 \sigma_{Max}} \exp\left(-\frac{\Delta E_1^a}{kT}\right), \tag{26}$$

$$e_1 = \frac{D_1}{a_1^2 C_1^{Sol}} \frac{\nu_i}{\nu_1} \exp\left(-\frac{\Delta E_1^a + G_1 - G_i}{kT}\right), \tag{27}$$

$$\frac{e_1}{t_1} \sim \frac{\sigma_{Max}}{a_1 C_1^{Sol}} \exp\left(-\frac{G_1 - G_i}{kT}\right), \tag{28}$$

where t_1 (e_1) is the trapping (emission) rate from (to) the material-1. Similarly, t_2 and e_2 can be defined by changing the subscript 1 to 2. For practical numerical simulation, it would be useful to treat $\nu_i/\nu_1 \sim 1$ and ΔE_1^a as a calibration factor.

At equilibrium ($J_1 = J_2 = 0$), the dilute limit approximation ($C_1 \ll C_1^{Sol}$ and $C_2 \ll C_2^{Sol}$) of Eq. 25 yields the same segregation ratio as the two-phase model.

$$C_1 = \frac{\sigma_i}{a_1} \frac{\nu_i}{\nu_1} \frac{C_1^{Sol} - C_1}{C_1^{Sol}} \frac{\sigma_{Max}}{\sigma_{Max} - \sigma_i} \exp\left(\frac{G_i - G_1}{kT}\right), \tag{29}$$

$$C_2 = \frac{\sigma_i}{a_2} \frac{\nu_i}{\nu_2} \frac{C_2^{Sol} - C_2}{C_2^{Sol}} \frac{\sigma_{Max}}{\sigma_{Max} - \sigma_i} \exp\left(\frac{G_i - G_2}{kT}\right), \tag{30}$$

$$\frac{C_2}{C_1} = \frac{a_1 \nu_1}{a_2 \nu_2} \exp\left(\frac{G_1 - G_2}{kT}\right), \tag{31}$$

$$\approx \exp\left(\frac{G_1 - G_2}{kT}\right) \tag{32}$$

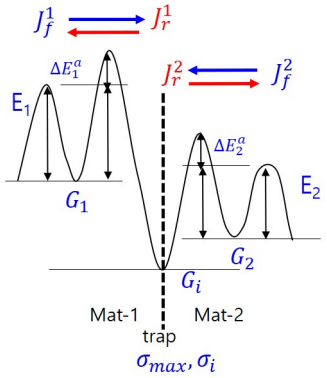

Fig. 4. Energy diagram for three-phase segregation parameters.

III. Applications and Discussions

We applied Eq. 13 to simulate boron (B) diffusion in strained $Si_{0.8}Ge_{0.2}$. Fig. 5 illustrates the sample structure and diffusion results. The five-stream diffusion model [4] was utilized to fit the secondary ion mass spectrometry (SIMS) data. Initially, B diffusivity was calibrated to fit the profile in the unstrained silicon region (the right side of the sample in Fig 5). Subsequently, the diffusion stress factor and the stress dependent drift term ($c_{eq}(x)$) were applied, which were based on the induced strain value at the transition state and the substitutional position, respectively. We employed $exp\left(-\frac{2.4e-29P}{kT}\right)$ as the diffusivity stress factor and $exp\left(\frac{1.8e-29P}{kT}\right)$ as the

c_{eq} in SI units, where P represents the pressure. Detailed descriptions of the induced strain values and methodology are provided in [5], [6].

Fig. 5 shows the effect of the $c^{eq}(x)$ term from Eq. 11. This term induces a drift when Ge concentration changes rapidly, causing B to segregate into the compressively strained $Si_{0.8}Ge_{0.2}$ region. In the absence of this term, the B profile is less abrupt at the edge of the Ge profile, as indicated by the dashed orange line in Fig. 5. If the simulation continues until the diffusion equilibrium state is reached, it will result in a step-like profile at the edge of the Ge profile. When additional position dependent free energy terms are present, Table I and Eq. 13 can properly describe the drift effects.

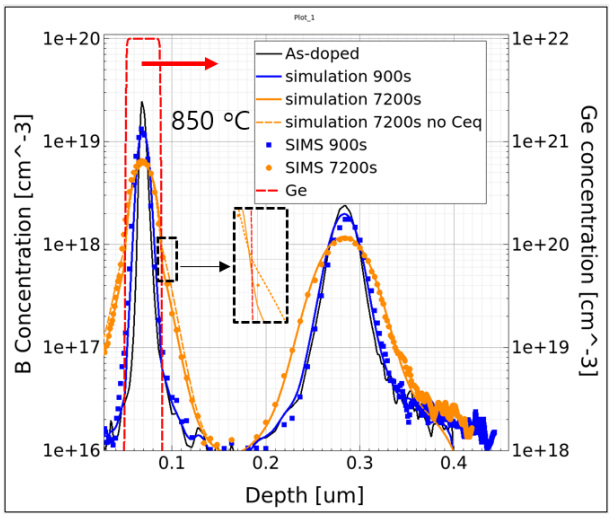

Fig. 5. B diffusion at 850°C. The inset is a magnified view near the edge of the Ge profile to visualize the effect of the generalized drift term (c_{eq}). The as-doped SIMS profile within the strained-$Si_{0.8}Ge_{0.2}$ region was scaled up by 5% to match the dose of the diffused profiles.

Usually, the two-phase segregation transfer rate is set to a large value compared to the rate determined by Eqs. 19 or 21. Fig. 6 shows an example of parameter values based on [7], [8]. When the transient behavior at the interface is not of interest, a large transfer rate is a safer choice, as a small value would cause exteremly slow evolution. However, when the transient segregation behavior is also important, Eq. 21 provides a baseline for determining the transfer rate with the additional calibration parameter ΔE^a. Although the example calculation of the two-phase segregation parameters was performed using boron parameters at the SiO_2/Si interface due to the limitation of available published data, the three-phase segregation model is usually employed for those cases [3] and the two-phase segregation model is more useful for scenarios where the interface trap is not explicitly simulated, such as hydrogen diffusion through the middle- or back-end-of-line stack.

Defining the trapping and emission rates of the three-phase segregation parameters has been even more challenging than for the two-phase segregation transfer rate because poorly defined parameter values outside of a reasonable range can cause convergence failures during simulations. Eqs. 27 and 28 offer a straightforward formula to determine baseline values for the trapping and emission rates using fundamental physical quantities. Note that G_i may include additional energy of a point defect if a point defect is involved in the trapping/emission process.

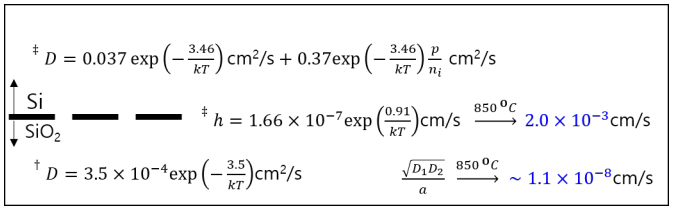

Fig. 6. Calculation example of two-phase segregation transfer rate using B parameters. The half of the silicon lattice constant was used as the value of a. ‡:Ref [7], †:Ref [8].

IV. Conclusion

Using the free energy diagram of the atomic movement, the Fick's first law was generalized to include all types of drift-inducing terms (e.g. electric potential energy, stress response energy, binding energy, TS). This approach is useful for describing continuous bulk segregation effects. Employing the same methodology, interface segregation parameters were formulated using tangible physical quantities, providing a straightforward method to define baseline values.

Acknowledgment

The SIMS data were obtained from FP6 European project (Grant No. 027152) ATOMICS.

References

[1] H. You, U. M. Gösele, and T. Y. Tan, "Simulation of the transient indiffusion-segregation process of triply negatively charged Ga vacancies in GaAs and AlAs/GaAs superlattices," J. Appl. Phys. vol.74, pp.2461-2470, 1993.

[2] D. A. Antoniadis, M. Rodoni, and R.W. Dutton, "Impurity redistribution in SiO2-Si during oxidation: A numerical solution including interfacial fluxes," J. Electrochem. Soc., vol.126, no.11, pp.1939-1945, 1979.

[3] Y.-S. Oh and D. E. Ward "A calibrated model for trapping of implanted dopants at material interface during thermal annealing," in IEDM Technical Digest, San Francisco, CA, USA, pp.509-512, December 1998.

[4] S.T. Dunham, "A quantitative model for the coupled diffusion of phosphorus and point defects in silicon," J. Electrochem. Soc., vol. 139, Issue 9, pp.2628-2636, 1992.

[5] C. Ahn, "Atomic scale modeling of stress and pairing effects on dopant behavior in silicon," Ph.D dissertation, University of Washington, Seattle, USA, 2007.

[6] ATOMICS final public report, "Advanced front-end technology modeling for ultimate integrated circuits," https://www.iisb.fraunhofer.de/content/dam/iisb2014/en/Documents/Research-Areas/Simulation/final-report-atomics.pdf, 2009.

[7] H. Puchner, "Advanced process modeling for VLSI technology," Ph.D dissertation, Vienna University of Technology, Vienna, Austria, 1996.

[8] C. Y. Wong and F. S. Lai, "Ambient and dopant effects on boron diffusion in oxides," Appl. Phys. Lett. vol.48, pp.1658-1660, 1986.